Check for updates

Microsatellite markers for *Monitipora digitata* designed using restriction-site associated DNA sequencing

Shuwen Jia*†, Yuanchao Li†, Shiquan Chen, Zefu Cai, Jie Shen, Yi Wang, Zhongjie Wu* and Daoru Wang*

Institute of Marine Ecology, Hainan Academy of Ocean and Fisheries Sciences, Haikou, China

Montipora digitata is a species belonging to the Acroporidae. In the Indo-Pacific region, *M. digitata* is widely distributed and is the dominant species of scleractinian coral in the South China Sea, however, there are currently no molecular markers suitable for assessing the species genetic diversity. Here, restriction-site associated DNA sequencing (RAD-seq) was used to isolate and characterize polymorphic microsatellite loci. A total of 317,361 RAD-tags were obtained using RAD-seq, including 6,778 microsatellite loci. Primer pairs for 106 loci were ordered and twenty-one polymorphic loci, that amplified reliably were identified. The number of alleles per locus were 2-7, observed heterozygosity was 0.111-0.556 with an average value of 0.285, and expected heterozygosity was 0.105- 0.802, with an average value of 0.536. Before Bonferroni correction 13 loci deviated significantly from the expectations of Hardy-Weinberg equilibrium ($P < 0.05$), after correction, two microsatellite loci deviated significantly ($P < 0.0002$). The polymorphic information content (PIC) ranged from 0.100-0.778, with 12 loci highly polymorphic (PIC > 0.5), six moderately polymorphic (0.25 < PIC < 0.5), and three loci with low polymorphism (PIC < 0.25). The microsatellite loci developed here will be effective tools for conservation genetic research on *M. digitata*.

KEYWORDS

South China Sea, scleractinian coral, polymorphic loci, genetic diversity, polymorphic information content

Introduction

Owing to the impact of global climate change and human activities, for example, sea surface temperature increases, China's coral reef ecosystem has declined rapidly, and coastal coral reefs cover has been reduced by at least 80% in the past 30 years (Hughes et al., 2012; Hughes et al., 2017). Scleractinian corals are an important component of coral reef ecosystems and studying the genetic structure and connectivity of scleractinian corals is important for the protection and restoration of coral reef ecosystems. However, there are

only a few studies on genetic diversity of scleractinian corals in the South China Sea (Wu et al., 2021) and microsatellite markers have been developed for some scleractinian corals such as *Porites lutea* (Hou, 2018; Li et al., 2020), *Pocillopora damicornis* (Luo et al., 2020), *Platygyra acuta* (Yang, 2013), *Galaxea fascicularis* (Su, 2017), distributed in the South China Sea. Previous studies have increased our understanding of scleractinian corals in the South China Sea, for example in *P. lutea*, it was found that there was genetic differentiation between Hainan Island and Xisha (Hou, 2018), and that seasonal differences in surface temperature at different latitudes might be driving genetic differentiation (Luo et al., 2022). However, there are many species of scleractinian coral in the South China Sea, and the understanding of the genetic diversity and genetic structure across scleractinian coral in the South China Sea is limited.

Montipora digitata (Dana, 1846) belongs to the family Acroporidae and is widely distributed in the South China Sea (Gu et al., 2017; Zhou et al., 2017). In recent years, field investigations in the South China Sea have found that *M. digitata* has replaced *P. lutea* as the dominant species in some areas, such as Dazhou Island of Wanning (Zhou et al., 2017). However, there are no molecular markers available for *M. digitata*, which makes up a growing proportion of South China Sea scleractinian corals.

Genetic work with scleractinian corals is difficult because they have symbiotic relationships with zooxanthellae. Because a large number of zooxanthellae live within the gastrodermal cells of the coral (Gleason and Wellington, 1993; Douglas, 2003). DNA extracted directly from coral tissue, will contain a large amount of zooxanthellae DNA. At present, the most commonly used method to separate the zooxanthellae from the coral hosts is to treat live coral at high temperatures, inducing the endosymbionts to leave the host, a process also known as bleaching (Li et al., 2020; Luo et al., 2020). Batch separation requires multiple sites and equipment that is not easy to operate and would not be an efficient step in preparing DNA for population genetic analysis. However, heat-induced bleaching can be performed using a small number of individual corals, and combined with bioinformatics methods, residual zooxanthellae DNA can be removed to obtain microsatellite markers of coral hosts. (Li et al., 2020; Luo et al., 2020). Restriction site-associated DNA sequencing (RAD-seq) greatly reduces the cost of genome sequencing and is not limited to the reference genome (Li et al., 2021; He et al., 2022).

In this study, *M. digitata* was bleached at high temperatures and RAD-seq was conducted to screen the coral for host-specific microsatellite. The new polymorphic microsatellite markers provide effective tools for obtaining genetic data useful for conservation.

Materials and methods

Coral samples for RAD-seq were collected from Luhuitou of Hainan Island (18.2167136, 109.4840218). The depths of the collection points were 2-10 m. A piece of live coral, approximately 5 cm long, was transported in seawater to the laboratory. After recovery in the indoor ocean simulation system, the coral was placed in a 43 cm^3

tank for heat bleaching treatment. After bleaching, it was frozen in liquid nitrogen and stored at -80 °C until DNA extraction. Tissues from nine corals were sampled from a population in Yinyu (16.58074097, 111.7079768) in the Xisha Islands and tissues from two individuals were sampled from Shiyu (16.54108719, 111.7526088) and Langhuajiao (16.46873192, 111.5773425) in the Xisha Islands, respectively. One tissue sample was collected from each reef, the interval between each reef was at least 2 m. Each tissue sample was approximately 2 cm in length and stored in absolute ethanol. After being transported back to the laboratory, tissues were it was stored in a refrigerator at -80 °C. Six individuals, including all individuals from Shiyu and Langhuajiao, and two randomly selected individuals from Yinyu were used for microsatellite discovery *via* RAD-seq and initial polymorphism screening.

Reduced-representation genome sequencing (RRGS) and microsatellite primer design

Artificial bleached coral tissue from Luhuitou was used for RAD-seq. RAD-seq-library generation and sequencing were completed in Genedenovo (Guangzhou, China). The CTAB method (Doyle and Doyle, 1987) was used to extract genomic DNA from each tissue sample and DNA quantity and quality were assessed using a NanoDrop 2000 (Thermo Fisher Scientific, Waltham, MA) and a Qubit (Thermo Fisher Scientific, Waltham, MA), as well as gel electrophoresis. Genomic DNA was digested using a restriction endonuclease (*Eco*RI) and P1 adapters with a unique 4-8 bp barcode sequence, were then ligated to DNA fragments using T4 ligase (NEB, Ipswich, MA, USA). Then DNA fragments were sheared randomly using a Branson Sonicator (model SX 30, Branson Ultrasonics, Danbury, CT, USA). The sheared DNA was purified, eluted and separated, and 300-700 bp corresponding DNA fragments were taken for purification by gel electrophoresis. Then, selected DNA fragments end were repaired, and dATP overhangs were added. Illumina sequencing adapters were added using NEBNext® ULtra™ DNA Library Prep Kit (NEB, USA), and PCR amplification and enrichment were performed. Finally, AMPure XP (Beckman Coulter, Brea, CA, USA) was used to purify the PCR products. Agilent 2100 biological analyzer (Agilent, Santa Clara, CA) was used to detect the sequencing library, and real-time PCR was used to quantify the library. Sequencing was carried out on NovaSeq 6000 sequencer using PE 150 sequencing strategy. Raw reads were processed to get high quality reads using fastp v. 0.18.0 (Chen et al., 2018) according to three stringent filtering standards: 1) remove reads where the proportion of N greater than 10%; 2) remove reads where the quality value of Q ater accounts for more than 50% of the whole read; and 3) remove reads aligned to the barcode adapter. Read1 were clustered using stack v. 1.46 (Catchen et al., 2011). Read2 were clustered according to the clustering result of read1, and then spliced. After splicing, the stack sequence with read1 and the conting sequence with read2 were aligned to the Symbiodiniaceae genome (*Symbiodinium microadriaticum*, Gonziodinium microadriaticu*Breviolum minutum*, Shoguchi et al., 2013; Beedessee et al., 2015; Shoguchi et al., 2015; *Symbiodinium kawagutii*, Lin et al., 2015) and the Symbiodiniaceae sequences removed. After filtering, the stack and conting sequences were spliced to construct RAD-tags to be used as reference sequences.

All reference sequences were searched using MISA software (http://pgrc.ipk-gatersleben.de/misa/) for microsatellite loci. The minimum repeat number of each motif was set as15, six, and five times for mono-, di-, and trinucleotide motifs, respectively; and four times for tetra-, penta-, and hexanucleotide motifs. When designing primers, adjacent microsatellite sequences that were separated by less than 100 bp were regarded as single microsatellite loci. Based on the flanking sequences at both ends of the microsatellites, primers for microsatellites were designed using Primer 3 v2.3.6 (http://primer3.sourceforge.net) under default settings, with the size of PCR products ranging from 100 to 300 bp. The universal FAM tail (GAAGGTGACCAAGTTCATGCT; Chao et al., 2022; Fan et al., 2023) was added to the 5' end of forward primers (Wuhan Tianyi Huayu Gene Technology Co., Ltd.). PCR amplification was performed in a total reaction volume of 25 μL that included 12.5μL 2 ×PCR Master Mix, 0.2μL forward primer (10μmol/L), 0.6 μL reverse primer (10μmol/L), 0.4μL FAM labeled primer (10μmol/L), 100ng template DNA, and finally supplemented with ddH$_2$O. Amplification was performed according to the following procedure: one cycle at 95 °C for 2min for initial denaturation, 30 cycles of: denaturation at 95 °C for 20sec, annealing at 50-55 °C for 20sec, and extension at 72 °C for 20sec, eight cycles of: denaturation at 95 °C for 20sec, annealing at 53 °C for 20sec, and extension at 72 °C for 30sec, and lastly a final extension at 72 °C for 5min.

PCR products with fluorescence labels were separated on an ABI 3730XL, and GeneMarker 3.0 used to identify genotypes. MicroChecker v.2.2.3 (Van Oosterhout et al., 2004) was used to check for genotyping errors and null alleles. The observed number of alleles (N_A), effective number of alleles (N_E), observed heterozygosity *(HO)*, expected heterozygosity *(HI)*, Shannon information index *(I)*, inbreeding coefficient within populations *(FIS)*, and Hardy-Weinberg equilibrium *(HWE)* were calculated using GenAlEx 6.5 (Peakall and Smouse, 2006). Linkage disequilibrium (LD) between each pair of loci was calculated using ARLEQUIN v3.5 (Excoffier and Lischer, 2010). Polymorphism information content (PIC) was calculated using PIC_CALC V. 0.6 (Germplasm Resources and Engineering Breeding Office, Yellow Sea Fisheries Research Institute, Chinese Academy of Fishery Sciences).

Results

After filtering, a total of 1,396,195,302 bp of high-quality data were generated by the Illumina NovaSeq6000 NGS platform (Table 1). After

excluding the data of Symbiodiniaceae, a total of 317,361 reference contigs for analysis were obtained using RAD-seq on the genome of *M. digitata*. The longest contigs was 2209 bp, shortest contigs was 157 bp, and average sequence length was 311 bp.

A total of 6,778 microsatellite loci were identified from the *M. digitata* data. Among them, 2,255 were trinucleotides, accounting for 33.27% of the total number of microsatellite loci, 1,705 were tetranucleotides, accounting for 25.15% of the total number. Dinucleotides, mononucleotides, pentanucleotides, and hexanucleotides had 1094, 719, 714, and 291 microsatellite loci, respectively, accounting for 16.14, 10.61, 10.53, and 4.29% of the total number, respectively (Table 2, Figure 1). The distribution of microsatellite repeat motifs in *M. digitata* is shown in Figure 2. Among the mononucleotides, the dominant motif was A/T, with 695, this accounted for 10.25% of the total number of microsatellite loci. In dinucleotides, the dominant motif was AT/AT, with 446, accounting for 6.58% of the total. Among the trinucleotides, the dominant repeat unit was AAT/ATT, with 712, accounting for 10.50% of the total. Among the tetranucleotides, AAAT/ATTT was the dominant motif, with 375, accounting for 5.53% of the total. Among the pentanucleotides, AAAGG/CCTTT was the dominant motif, with 93, and 1.37% of the total number of microsatellite loci. Among the hexanucleotides, AACCCT/AGGGTT was the dominant motif, with 38, accounting for 0.56% of the total number of microsatellite loci. One hundred and six microsatellite primers with PCR products of approximately 200 bp were randomly selected, and polymorphism was assessed for each locus using six individuals. Thirty-seven pairs of primers could be amplified clearly and were polymorphic. Finally, 21 highly polymorphic loci were selected for genetic analysis using nine tissue from Yinu (Table 3, Figure 3). The presence of null alleles at a nine loci (Table 4). The number of alleles per locus ranged from 2–7, *H*o was 0.111-0.556, and *H*$_E$ was 0.111-0.802. Twelve loci were highly polymorphic (PIC > 0.5), six were moderately polymorphic (0.25 < PIC < 0.5), and three were less polymorphic (PIC < 0.25). Before Bonferroni correction 13 loci deviated significantly from the expectations of Hardy-Weinberg equilibrium ($P < 0.05$), after correction, two microsatellite loci deviated significantly ($P < 0.0002$). The linkage disequilibrium analysis of 21 SSR marker loci showed there were 18 pairs of paired points with significant linkage disequilibrium out of 210 total comparisons (8.57%, Table 5). See Table 6 for full summary of genetic diversity.

TABLE 1 Summary of genomic sequences generated by RAD-seq.

Before data filtering					After data filtering				
Clean Data (bp)	Q20 (%)	Q30 (%)	N (%)	GC (%)	HQ Clean Data (bp)	HQ Q20 (%)	HQ Q30 (%)	HQ N (%)	HQ GC (%)
1423400136	1366681891 (96.02%)	1276795857 (89.7%)	4667 (0.0%)	563350809 (39.58%)	1396195302	1343251931 (96.21%)	1255475986 (89.92%)	4457 (0.0%)	551312001 (39.48%)

Clean Data: total base number of offline data; HQ Clean Data: total number of high-quality data bases after filtering; Q20 (%): the number of bases with the quality value of sequenced bases reaching the level of Q20 (sequencing error rate of 1%) and the percentage in RawData (or CleanData); Q30 (%): number of bases with the quality value of sequenced bases reaching the level of Q30 (sequencing error rate of 0.1%) and the percentage in Raw Data (or Clean Data); N (%): the number of N-base in single-end read and its percentage in Raw Data (or Clean Data); GC (%): percentage of sequence base GC before (after) filtration.

TABLE 2   SSR motif information statistics of *M. digitata*.

Total number of sequences examined:	317361
Total size of examined sequences (bp):	98730250
Total number of identified SSRs:	6778
Number of SSR containing sequences:	6235
Number of sequences containing more than 1 SSR:	457
Number of SSRs present in compound formation:	470
Mononucleotide	719
Dinucleotide	1094
Trinucleotide	2255
Tetranucleotide	1705
Pentanucleotide	714
Hexanucleotide	291

Discussion

In this study, 6,778 microsatellite loci were detected from RAD-seq data of *M. digitata*, with a distribution frequency of 2.14%. This distribution frequency was similar to that of *Parus palustris* (2.2%; Wan et al., 2016), *Patinopecten yessoensis* (1.4%; Ni et al., 2018), and *Clematis* (2.11%; Song et al., 2022) but was much lower than those of *Datnioides pulcher* (16.1%; Qu et al., 2019) and *Pelteobagrus vachellii* (20.52%; Wang et al., 2021). This indicates a significant

difference in the abundance of microsatellites among different species. This result is consistent with the findings of Liu et al. (2021).

The microsatellite loci of *M. digitata* are dominated by trinucleotides, followed by tetranucleotides, which is consistent with results reported for other cnidarians. Ruiz-Ramos and Baums (2014) studied 11 species of cnidarians and found that the highest abundance of microsatellites in Anthozoa and Hydrozoa were trinucleotides and tetranucleotides. This is similar to the distribution of microsatellite loci in other invertebrates. Among the 33 animal species counted in this study (Table 7), the dominant microsatellite motif of most invertebrates is mainly mononucleotides (*Tenebrio molitor*, Zhu et al., 2013; *Phenacoccus Solenopsis*, Luo et al., 2014;*Galeruca daurica*; Zhang et al., 2016), dinucleotides (*Exopalaemon carinicauda*, Duan et al., 2016) or trinucleotides (*Eucryptorrhynchus chinensis*, Wu et al., 2016; *Tetranychus dichromata*, Wang et al., 2013). However, it is significantly different from that of vertebrates, which are dominated by mononucleotides and dinucleotides (Qi et al., 2015; Tang et al., 2022).

The dominant motifs of mononucleotides, dinucleotides, trinucleotides, and tetranucleotides in *M. digitata* are A\T, AT \AT, AAT\ATT, and AAAT\ATTT, respectively, similar to previous microsatellite distribution research results (Wang et al., 2013; Jo et al., 2021; Su et al., 2021). In mononucleotides, A\T is the dominant motif of most species (Wang et al., 2013; Luo et al., 2014; Qi et al., 2015; Wu et al., 2016; Liu et al., 2021; Su et al., 2021). Among dinucleotides, AC is the most common motif, however, AT is also common in invertebrates such as *Ixodes scapularis* (Wang et al., 2013), *E.chinensis* (Wu et al., 2016), *P.yessoensis* (Ni et al.,

FIGURE 1
(A) The proportion of different motifs of microsatellites in *M. digitata*. (B) The production of difference motifs of total length of microsatellites in *M. digitata*. (C) Distribution of number of base repetitions of microsatellites repeat motifs in *M. digitata*.
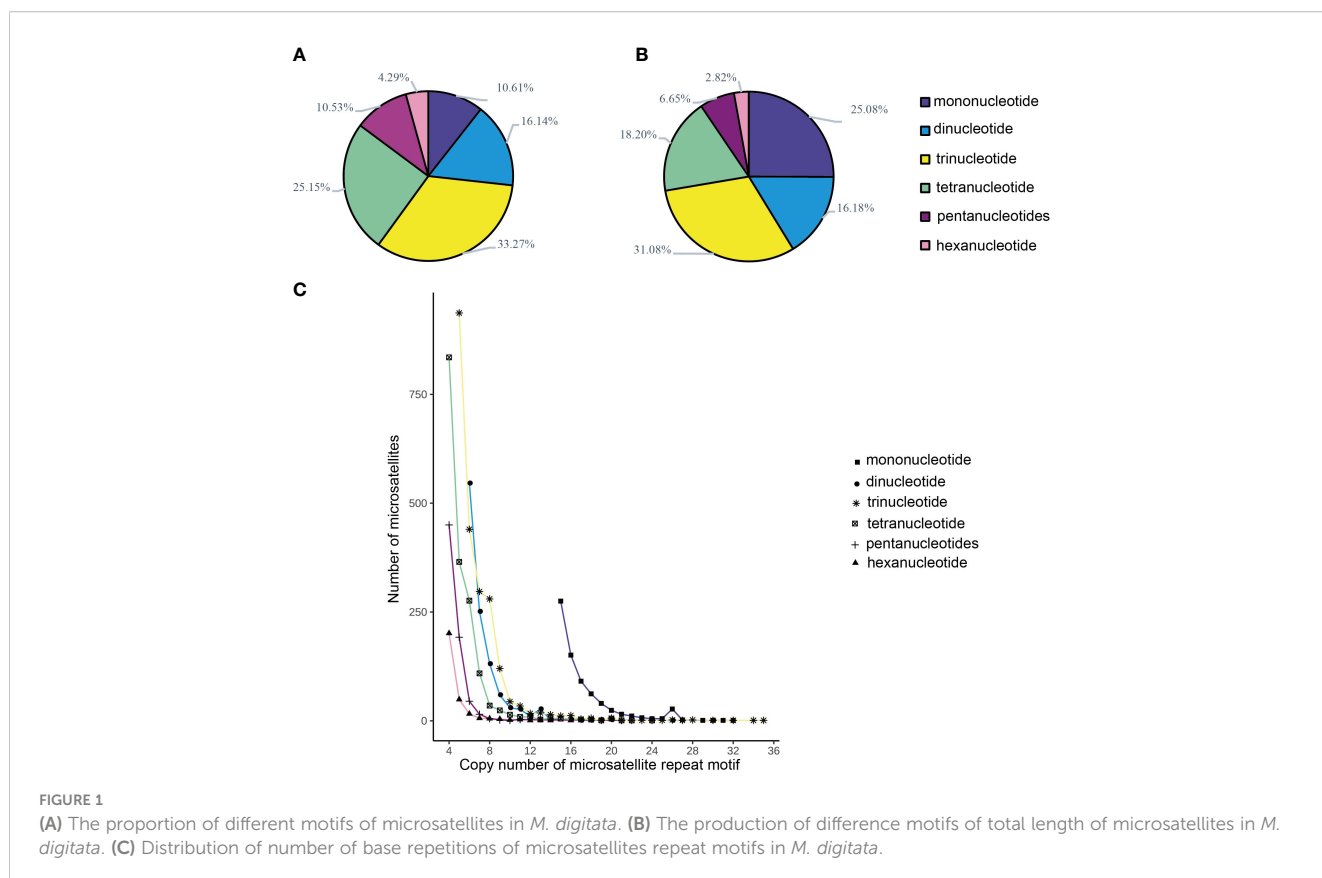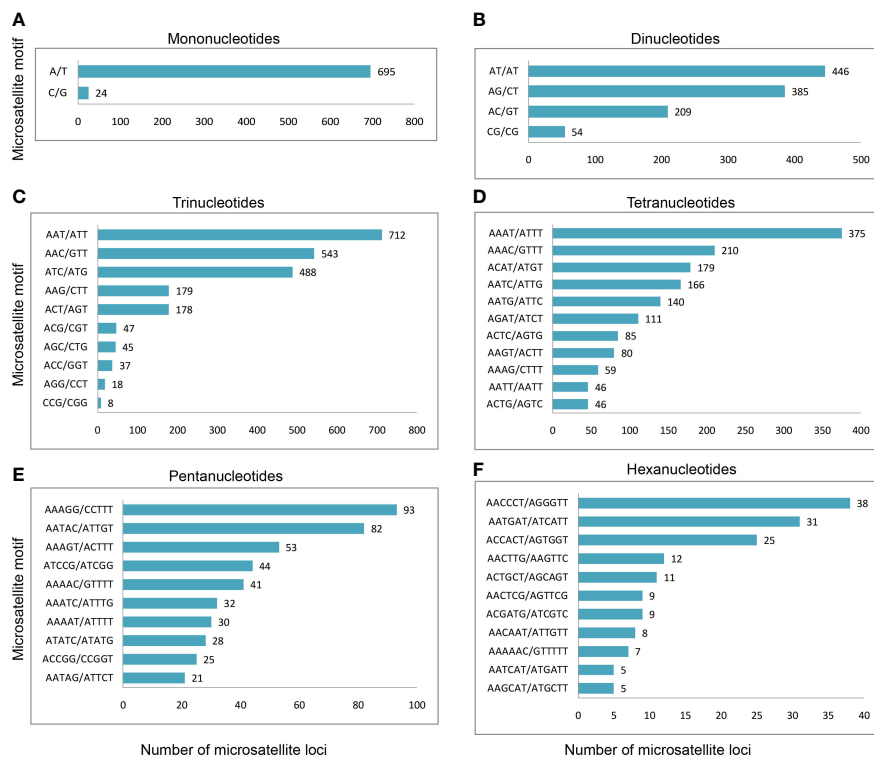
FIGURE 2
The distribution of microsatellite motifs in *M. digitata*. **(A–F)** The distribution of microsatellite motifs in the mono-, di-, tri-, tetra-, penta-, and hexanucleotide motif, respectively. Only the top ten repeat motifs are shown in **(D–F)**. The number after the column represents the number of repeat motifs.

TABLE 3 Twenty one pairs of microsatellites primer information.

Locus	Repeat motif	Forward primer (5'-3')	Reverse primer (5'-3')	Product size (bp)
ZH10002	(TCA)7	CTGTCCGTGCAAAGAACAAC	CAAAGTTGCCTGGAAGGAAG	222
ZH10127	(CGTCA)5	TCAAACCGATTCCTTTCCTG	AAGCAGCTACCACGTTCCAC	220
ZH11510	(TA)8(GA)7	TAAAAAGGCGTGCTCACAGA	TGTTAACAGCGAGGGTATTGG	254
ZH11934	(AAT)7	TTCTCTTAAATCGACAAAAAGAAGT	CCAGTACCATGGGCAGTTTT	220
ZH12347	(GAA)6gcaga(AGG)6	AAAAGCAAAACAGGCACCAT	AAAATCACAGATAGTCTGCAAGAAAA	223
ZH12502	(TCA)6	TCATCGTCGTCATCATCGTT	TCGCCAAAATTCAAGGTAGG	246
ZH12756	(TTTA)4	GAGCAGTGAAGATGGCTTCC	TTTGGGCTTGTGATTGTTCA	198
ZH12912	(GTGA)10	GGTTGTTCACTTTTTGCGGT	CACTTCCAACGGACCTGTTT	197
ZH13293	(TCAAGT)4	AATTACCCCGGCTTCGTAGT	GCTAGCTCTGTTTTCAGTTTCTTTTT	216
ZH13301	(GT)6	TTGATAACCAGTGGCAGGCT	ACCTGTGGTGCGAGATTTTC	203
ZH13561	(TTG)7	TTTTGCGTCGGTATCAAAGA	GCAATTTATTGGACACGCCT	225
ZH13573	(TC)6	TTCGCCTTCGAAATCTCATC	CGAAAGGAGCCTGGTTAGAA	241
ZH14680	(AAAT)4	CTTGCATTTTTCCCTGCTGT	TGCTGTCACATTTCAATGCC	270
ZH15503	(AG)7	CTCTAAAACCCGCAGACCAC	CATGACGGCGCTCATACATA	257
ZH15709	(TGT)5	CTAGCACCTGCTATTTGCGG	GCGAAGATCGTGGAAACAAA	266
ZH17044	(CAA)5	TGTCCTGGCCATGAACATTA	TCGATTTTCGATTAAACCACC	250
ZH18332	(TATT)6	ACCACTTAGGCTTCTGCACG	GGGGGAGAGAAAAATGTCGT	219

(Continued)

TABLE 3 Continued

Locus	Repeat motif	Forward primer (5'-3')	Reverse primer (5'-3')	Product size (bp)
ZH18580	(CACG)6	CAACGAAACTCGACCCTCAT	GCAGAAATGAAGATGCCACA	209
ZH20640	(T)15	AGGGCTGGGCTCTAGTGAAT	AGTAGAAGGTGGCACACGGT	205
ZH21554	(AAGT)7	CCAATCGGGGCTACTATGAA	CGTGCACGTTCTCACTAGTTTT	254
ZH21810	(AT)7	TGAATGCGAAATGCGAAGTA	AGGCTTGAAGAGTACCCCGT	275

2018), and *Artemia franciscana* (Jo et al., 2021). AAT\ATT and AAAT\ATTT are also common trinucleotide and tetranucleotide motifs, respectively, such as those in *A.franciscana* (Jo et al., 2021), *I.scapularis* (Wang et al., 2013), *Boa constrictor*, and *Protobothrops mucrosquamatus* (Nie et al., 2017). This shows that dominant motifs of *M. digitata* are similar to what is seen in most species. Previous studies that used transcriptome data to develop microsatellite loci also found fewer GC motifs, presumably due to the methylation of cytosine in CpG sequences important for the regulation of transcription (Gonzalez-Ibeas et al., 2007; Xing et al., 2017; Liu et al., 2021).

Microsatellites are among the most commonly used molecular markers for genetic diversity analysis. However, traditional methods to

develop microsatellite markers are tedious and have a low success rate. For example, to develop SSR markers using standard enrichment protocols requires the construction of microsatellite enrichment libraries, hybridization, and sequencing, which requires a large amount of experimental work expertise and high cost (Jia et al., 2013; Jia and Zhang, 2019). With the development of high-throughput sequencing, microsatellite marker development based on transcriptome and RRGS data have emerged. RRGS has been widely used as follows: specific-locus amplified fragment sequencing (SLAF-seq) and RAD-seq, of which RAD-seq is the more widely used. Compared with SLAF-seq, RAD-seq can obtain more markers, and the splicing of read2 may result in longer fragments, which is often used in the development of high-density and microsatellite markers (Wang
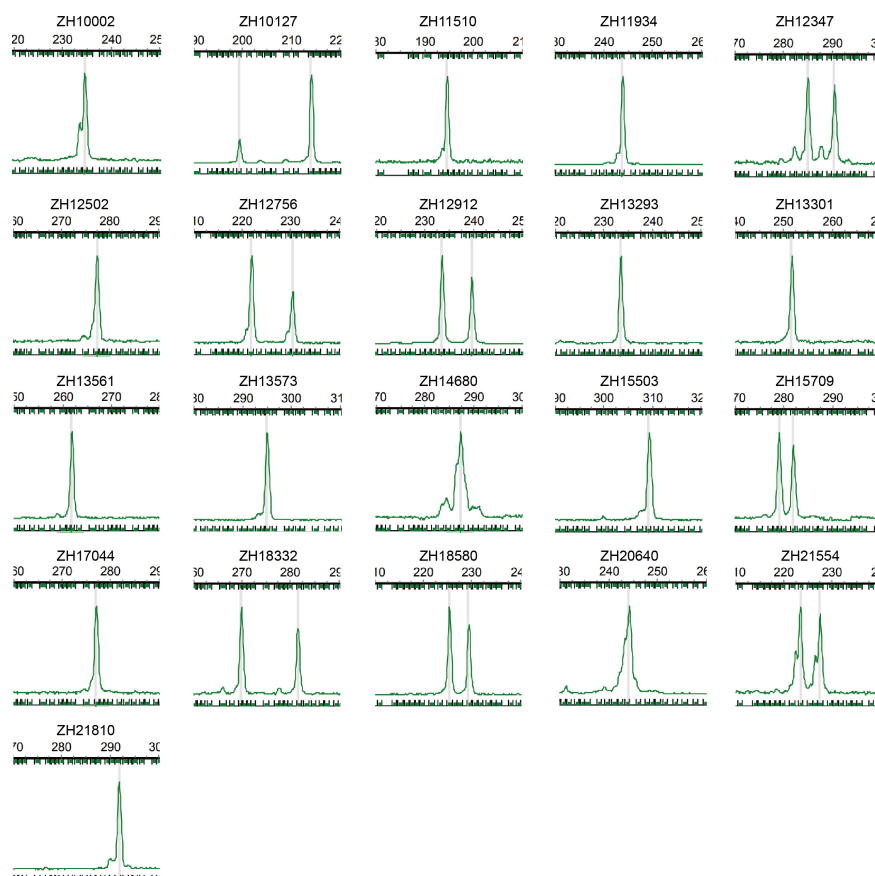
FIGURE 3

Peak diagram of capillary electrophoresis detection of 21 pairs of primers of *M. digitata*.

TABLE 4 Results of null alleles at 21 microsatellite loci.

Locus	Null Present	Oosterhout	Chakraborty	Brookfield 1	Brookfield 2
ZH10002	yes	0.337	0.621	0.247	0.247
ZH10127	no	0.139	0.182	0.120	0.120
ZH11510	no	0.128	0.135	0.100	0.100
ZH11934	no	0.150	0.200	0.133	0.133
ZH12347	no	0.154	0.174	0.123	0.311
ZH12502	yes	0.369	0.676	0.294	0.294
ZH12756	yes	0.337	0.644	0.265	0.265
ZH12912	yes	0.221	0.287	0.199	0.199
ZH13293	no	-0.333	-0.161	-0.110	0.000
ZH13301	no	-0.057	-0.029	-0.006	0.000
ZH13561	yes	0.243	0.353	0.215	0.215
ZH13573	yes	0.251	0.383	0.237	0.237
ZH14680	no	-0.057	-0.029	-0.006	0.000
ZH15503	no	-0.184	-0.091	-0.044	0.000
ZH15709	no	0.093	0.122	0.065	0.065
ZH17044	yes	0.365	0.692	0.310	0.310
ZH18332	no	0.156	0.171	0.128	0.128
ZH18580	no	0.092	0.058	0.042	0.042
ZH20640	no	0.155	0.200	0.111	0.111
ZH21554	yes	0.219	0.303	0.179	0.179
ZH21810	yes	0.337	0.644	0.265	0.265

TABLE 5 Significance test of 21 microsatellite linkage disequilibrium.

Locus	Locus	P–Value	Locus	Locus	P–Value	Locus	Locus	P–Value
ZH10002	ZH10127	0.00013	ZH12347	ZH14680	0.46803	ZH12347	ZH18580	0.00827
ZH10002	ZH11510	0.01033	ZH12502	ZH14680	0.74762	ZH12502	ZH18580	0.00477
ZH10127	ZH11510	0.00299	ZH12756	ZH14680	0.59985	ZH12756	ZH18580	0.0007
ZH10002	ZH11934	0.00013	ZH12912	ZH14680	0.55004	ZH12912	ZH18580	0.02808
ZH10127	ZH11934	0.00013	ZH13293	ZH14680	0.24813	ZH13293	ZH18580	0.09874
ZH11510	ZH11934	0.00211	ZH13301	ZH14680	0.73153	ZH13301	ZH18580	0.74762
ZH10002	ZH12347	0.00348	ZH13561	ZH14680	0.5092	ZH13561	ZH18580	0.01411
ZH10127	ZH12347	0.00063	ZH13573	ZH14680	0.29231	ZH13573	ZH18580	0.02964
ZH11510	ZH12347	0.02951	ZH10002	ZH15503	0.01739	ZH14680	ZH18580	0.74762
ZH11934	ZH12347	0.00096	ZH10127	ZH15503	0.01923	ZH15503	ZH18580	0.00718
ZH10002	ZH12502	0.00083	ZH11510	ZH15503	0.03396	ZH15709	ZH18580	0.27994
ZH10127	ZH12502	0.00041	ZH11934	ZH15503	0.01923	ZH17044	ZH18580	0.00048
ZH11510	ZH12502	0.01568	ZH12347	ZH15503	0.09522	ZH18332	ZH18580	0.02765

(Continued)

TABLE 5 Continued

Locus	Locus	P–Value	Locus	Locus	P–Value	Locus	Locus	P–Value
ZH11934	ZH12502	0.00046	ZH12502	ZH15503	0.04807	ZH10002	ZH20640	0.00325
ZH12347	ZH12502	0.00773	ZH12756	ZH15503	0.01923	ZH10127	ZH20640	0.00303
ZH10002	ZH12756	0.00013	ZH12912	ZH15503	0.06061	ZH11510	ZH20640	0.00642
ZH10127	ZH12756	0.00008	ZH13293	ZH15503	0.14028	ZH11934	ZH20640	0.00098
ZH11510	ZH12756	0.00155	ZH13301	ZH15503	0.53963	ZH12347	ZH20640	0.00709
ZH11934	ZH12756	0.00013	ZH13561	ZH15503	0.00718	ZH12502	ZH20640	0.00357
ZH12347	ZH12756	0.00168	ZH13573	ZH15503	0.0169	ZH12756	ZH20640	0.0014
ZH12502	ZH12756	0.00008	ZH14680	ZH15503	0.53963	ZH12912	ZH20640	0.01745
ZH10002	ZH12912	0.02676	ZH10002	ZH15709	0.29042	ZH13293	ZH20640	0.01327
ZH10127	ZH12912	0.01479	ZH10127	ZH15709	0.16135	ZH13301	ZH20640	0.80831
ZH11510	ZH12912	0.06496	ZH11510	ZH15709	0.21714	ZH13561	ZH20640	0.17313
ZH11934	ZH12912	0.00601	ZH11934	ZH15709	0.15175	ZH13573	ZH20640	0.13199
ZH12347	ZH12912	0.02471	ZH12347	ZH15709	0.18919	ZH14680	ZH20640	0.22931
ZH12502	ZH12912	0.01361	ZH12502	ZH15709	0.11498	ZH15503	ZH20640	0.02908
ZH12756	ZH12912	0.00766	ZH12756	ZH15709	0.11827	ZH15709	ZH20640	0.47306
ZH10002	ZH13293	0.08334	ZH12912	ZH15709	0.16089	ZH17044	ZH20640	0.00117
ZH10127	ZH13293	0.03827	ZH13293	ZH15709	0.50313	ZH18332	ZH20640	0.00525
ZH11510	ZH13293	0.25831	ZH13301	ZH15709	0.19934	ZH18580	ZH20640	0.00132
ZH11934	ZH13293	0.08313	ZH13561	ZH15709	0.02814	ZH10002	ZH21554	0.00083
ZH12347	ZH13293	0.0375	ZH13573	ZH15709	0.02155	ZH10127	ZH21554	0.00053
ZH12502	ZH13293	0.05999	ZH14680	ZH15709	0.04205	ZH11510	ZH21554	0.01177
ZH12756	ZH13293	0.04707	ZH15503	ZH15709	0.33708	ZH11934	ZH21554	0.00024
ZH12912	ZH13293	0.18552	ZH10002	ZH17044	0.00013	ZH12347	ZH21554	0.00143
ZH10002	ZH13301	0.65703	ZH10127	ZH17044	0.00013	ZH12502	ZH21554	0.00401
ZH10127	ZH13301	0.39869	ZH11510	ZH17044	0.00398	ZH12756	ZH21554	0.00064
ZH11510	ZH13301	0.27472	ZH11934	ZH17044	0.00013	ZH12912	ZH21554	0.03147
ZH11934	ZH13301	0.62779	ZH12347	ZH17044	0.00087	ZH13293	ZH21554	0.05562
ZH12347	ZH13301	0.6057	ZH12502	ZH17044	0.00048	ZH13301	ZH21554	0.69499
ZH12502	ZH13301	0.09628	ZH12756	ZH17044	0.0001	ZH13561	ZH21554	0.02948
ZH12756	ZH13301	0.04205	ZH12912	ZH17044	0.00536	ZH13573	ZH21554	0.03377
ZH12912	ZH13301	0.55004	ZH13293	ZH17044	0.07532	ZH14680	ZH21554	0.09628
ZH13293	ZH13301	0.41194	ZH13301	ZH17044	0.4855	ZH15503	ZH21554	0.04807
ZH10002	ZH13561	0.03502	ZH13561	ZH17044	0.00105	ZH15709	ZH21554	0.0502
ZH10127	ZH13561	0.03292	ZH13573	ZH17044	0.00431	ZH17044	ZH21554	0.00035
ZH11510	ZH13561	0.036	ZH14680	ZH17044	0.4855	ZH18332	ZH21554	0.00825
ZH11934	ZH13561	0.03775	ZH15503	ZH17044	0.01923	ZH18580	ZH21554	0.0003
ZH12347	ZH13561	0.0256	ZH15709	ZH17044	0.06352	ZH20640	ZH21554	0.00119
ZH12502	ZH13561	0.00404	ZH10002	ZH18332	0.00718	ZH10002	ZH21810	0.00013
ZH12756	ZH13561	0.00772	ZH10127	ZH18332	0.00533	ZH10127	ZH21810	0.00008

(Continued)

TABLE 5 Continued

Locus	Locus	P–Value	Locus	Locus	P–Value	Locus	Locus	P–Value
ZH12912	ZH13561	0.01208	ZH11510	ZH18332	0.12313	ZH11510	ZH21810	0.00155
ZH13293	ZH13561	0.20554	ZH11934	ZH18332	0.00477	ZH11934	ZH21810	0.00013
ZH13301	ZH13561	0.17538	ZH12347	ZH18332	0.00879	ZH12347	ZH21810	0.00168
ZH10002	ZH13573	0.09412	ZH12502	ZH18332	0.03709	ZH12502	ZH21810	0.00008
ZH10127	ZH13573	0.07951	ZH12756	ZH18332	0.00663	ZH12756	ZH21810	0.00001
ZH11510	ZH13573	0.02726	ZH12912	ZH18332	0.18372	ZH12912	ZH21810	0.00766
ZH11934	ZH13573	0.02836	ZH13293	ZH18332	0.09161	ZH13293	ZH21810	0.04707
ZH12347	ZH13573	0.03055	ZH13301	ZH18332	0.80371	ZH13301	ZH21810	0.04205
ZH12502	ZH13573	0.0193	ZH13561	ZH18332	0.02702	ZH13561	ZH21810	0.00772
ZH12756	ZH13573	0.02561	ZH13573	ZH18332	0.02089	ZH13573	ZH21810	0.02561
ZH12912	ZH13573	0.01363	ZH14680	ZH18332	0.27472	ZH14680	ZH21810	0.59985
ZH13293	ZH13573	0.33354	ZH15503	ZH18332	0.11112	ZH15503	ZH21810	0.01923
ZH13301	ZH13573	0.29231	ZH15709	ZH18332	0.06901	ZH15709	ZH21810	0.11827
ZH13561	ZH13573	0.00004	ZH17044	ZH18332	0.00054	ZH17044	ZH21810	0.0001
ZH10002	ZH14680	0.65703	ZH10002	ZH18580	0.00076	ZH18332	ZH21810	0.00663
ZH10127	ZH14680	0.39869	ZH10127	ZH18580	0.00069	ZH18580	ZH21810	0.0007
ZH11510	ZH14680	0.42182	ZH11510	ZH18580	0.01033	ZH20640	ZH21810	0.0014
ZH11934	ZH14680	0.31389	ZH11934	ZH18580	0.00039	ZH21554	ZH21810	0.00064

TABLE 6 Characteristics of 21 newly developed polymorphic microsatellite markers in *M. digitata*.

Locus	N_A	N_E	I	H_O	H_E	F_{IS}	PIC	p (HWE)
ZH10002	3.000	1.906	0.787	0.111	0.475	0.766	0.404	0.025*
ZH10127	3.000	2.793	1.061	0.444	0.642	0.308	0.568	0.010*
ZH11510	6.000	3.682	1.523	0.556	0.728	0.237	0.695	0.024*
ZH11934	3.000	3.000	1.099	0.444	0.667	0.333	0.593	0.019*
ZH12347	4.000	3.459	1.305	0.500	0.711	0.297	0.658	0.133
ZH12502	4.000	2.348	1.014	0.111	0.574	0.806	0.500	0.000**
ZH12756	3.000	2.051	0.828	0.111	0.512	0.783	0.426	0.028*
ZH12912	7.000	5.063	1.773	0.444	0.802	0.446	0.778	0.000**
ZH13293	2.000	1.670	0.591	0.556	0.401	-0.385	0.321	0.249
ZH13301	2.000	1.117	0.215	0.111	0.105	-0.059	0.100	0.860
ZH13561	4.000	3.306	1.276	0.333	0.698	0.522	0.642	0.003*
ZH13573	5.000	3.951	1.488	0.333	0.747	0.554	0.709	0.001*
ZH14680	2.000	1.117	0.215	0.111	0.105	-0.059	0.100	0.860
ZH15503	2.000	1.385	0.451	0.333	0.278	-0.200	0.239	0.549
ZH15709	3.000	1.742	0.730	0.333	0.426	0.217	0.371	0.719
ZH17044	3.000	2.571	1.011	0.111	0.611	0.818	0.536	0.008*
ZH18332	6.000	4.629	1.648	0.556	0.784	0.291	0.753	0.015*

(Continued)

TABLE 6 Continued

Locus	N_A	N_E	I	H_O	H_E	F_{IS}	PIC	p (HWE)
ZH18580	4.000	2.656	1.168	0.556	0.623	0.109	0.579	0.005*
ZH20640	2.000	2.000	0.693	0.333	0.500	0.333	0.375	0.317
ZH21554	4.000	2.656	1.117	0.333	0.623	0.465	0.557	0.125
ZH21810	3.000	2.051	0.828	0.111	0.512	0.783	0.426	0.028*
Mean	3.375	2.523	0.947	0.285	0.536	0.432		

N_A, observed number of alleles; N_E, effective number of alleles; H_O, observation of heterozygosity; H_E, expected heterozygosity; I, Shannon information index; PIC, polymorphism information content; F_{IS}, inbreeding coefficient within populations; p(HWE), probability of Chi-square test for Hardy-Weinberg equilibrium; *, significant departure from expected Hardy-Weinberg equilibrium before Bonferroni correction (p < 0.05); **, significant departure from expected Hardy-Weinberg equilibrium after Bonferroni correction (p < 0.0002).

TABLE 7 Statistics of microsatellite characteristics of 33 published studies.

Species	Base number of dominant motif	The most common SSR motifs of six different repeat types						The identification criteria minimum number of repeat times	References
		Mono-	Di-	Tri-	Tetra-	Penta-	Hexa-		
Vertebrate									
Ictalurus punctatus	Mono-	A	AC	AAT	AAAT	ATAAT	TGACTA	10,6,5,5,5,5	Tang et al., 2022
Bagarius yarrelli	Mono-	A	AC	AAT	ATAG	AATCT	AACCCT	10,6,5,5,5,5	Yang et al., 2021
Ctenopharyngodon idella	Mono-	A	AC	AAT	AGAT	AATAT	AACCCT	10,6,5,5,5,5	Huang et al., 2022
Mugilogobius chulae	Mono-	A	AG	AGC				12,6,5,5,4,4	Cai et al., 2015
Takifugu rubripes	Mono-	A	AC	AGG	ACCT	AGAGG	TTAGGG	10,6,5,5,5,5	Xu et al., 2021a
T. flavidus	Mono-	A	AC	AGG	AGGT	AGAGG	AACCCT	10,6,5,5,5,5	Xu et al., 2021a
T. bimaculatus	Mono-	A	AC	AGG	ACAG	AGAGG	TTAGGG	10,6,5,5,5,5	Xu et al., 2021a
Tetraodon nigroviridis	Mono-	A	AC	AGG	ATCT	AAGAT	AACCCT	10,6,5,5,5,5	Xu et al., 2021a
Placocheilus cryptonemus	Mono-	A	AC	AGG	AGAT	AGAGG	AAAGAC	10,6,5,5,5,5	Ren and Ma, 2021
Pelteobagrus vachelli	Di-	A	AC	AAT	AAAT	AATCT	GGGTTA	10,6,5,5,5 ,5	Peng et al., 2022
Ageneiosus marmoratus	Di-	A	AT	AAT	AAAT	AATAT	AAATGT	10,6,5,5,5,5	Su et al., 2021
Scatophagus argus	Di-	A	AC	AGG	AGAT	AGAGG	AATCAG	10,6,5,5,5 ,5	Wang et al., 2020
Pelteobagrus fulvidraco	Di-	A	AC	AAT	AAAT	AATCT	AACCCT	10,6,5,5,5 ,5	Xu et al., 2020
Acanthogobius ommaturus	Tri-		AT	ATT	CATG	AATTC	TTCTGA	-,6,4,4,4 ,4	Song et al., 2020
Boa constrictor	Mono-	A	AC	AAT	AAAT	AAAAT	ACATAT	12,7,5,4,4,4	Nie et al., 2017
Protobothrops mucrosquamatus	Mono-	A	AC	AAT	AAAT	AATAG	ACATAT	12,7,5,4,4,4	Nie et al., 2017

(Continued)

TABLE 7 Continued

Species	Base number of dominant motif	The most common SSR motifs of six different repeat types						The identification criteria minimum number of repeat times	References
Arborophila rufipectus	Mono-	A	AC	AAC	AAAC	AAACA	AGGGTT	12,7,5,4,4,4	Huang et al., 2015
Macaca fascicularis	Mono-	A	AC	AAT	AAAT	AAACA	AAACAA	12,7,5,4,4,4	Tu et al., 2018
Ailuropoda melanoleuca	Mono-	A	AC	AAT	AAAT	AAACA	AAACAA	12,7,5,4,4,4	Li et al., 2014
Ursus maritimus	Mono-	A	AC	AAC	AAAT	AAACA	AAACAA	12,7,5,4,4,4	Li et al., 2014
Pantholops hodgsonii	Mono-	A	AC	AGC	AAAT	AACTG	AAAGTG	12,7,5,4,4,4	Qi et al., 2016
Capra hircus	Mono-	A	AC	AGC	AAAT	AACTG	AAACAA	12,7,5,4,4,4	Qi et al., 2016
Invertebrate									
Sepiella japonica	Mono-	A	AT	AAT	AAAG			12,6,5,5,4,4	Sun et al., 2019
Eriocheir sinensis	Mono-	A	AC	AGG	AAGG	AACCT	AAGAGG	10,6,5,5,5,5	Xu et al., 2021b
Phenacoccus solenopsis	Mono-	A	AC	AAC	AAAG	AATCG		12,6,5,5,4,4	Luo et al., 2014
Anopheles sinensis	Mono-	A	AC	AGC	AAAT	AACCT	AACAGC	10,6,5,5,5,5	Wang et al., 2016
Ixodes scapularis	Mono-	A	AT	AAT	AAAT	AAATG	ACGCCG	12,7,5,4,4,4	Wang et al., 2013
Eucryptorrhynchus chinensis	Tri-	A	AT	TTA	ATAA	AGGTT		12,6,5,5,5,5	Wu et al., 2016
Tomicus yunnanensis	Tri-	A	AC	AAC	AAAT			12,6,5,5,4,4	Yuan et al., 2014
Tetranychus urticae	Tri-	A	AC	ATC	AAAT	AACCT	AAGATG	12,7,5,4,4,4	Wang et al., 2013
Patinopecten yessoensis	Tri-		AT	ATA	CAAA	AAACC		Minimum length of SSR motifs is 12	Ni et al., 2018
Artemia franciscana	Di-		AT	AAT	AAAT	AATAT	AGAGCC	-,5,5,5,5,5	Jo et al., 2021
Apis mellifera ligustica	Di-		AT	AAT	AAAG	AAAAG		-,6,5,5,5,5	Guo et al., 2018

Mono-, Mononucleotide; Di-, Dinucleotide; Tri-, Trinucleotide; Tetra-, Tetranucleotide; Penta-, Pentanucleotide; Hexa-, Hexanucleotide.

et al., 2012; Sun et al., 2013; Wang et al., 2014; Andrews et al., 2016). In addition, transcriptome sequencing data are widely used to develop EST-SSR (He et al., 2020; Liu et al., 2021). EST-SSRs are derived from transcribed regions of genes, and compared with genome SSR markers, more conserved, but they may be used to identify alleles associated with significant traits (Chen et al., 2017; Karcı et al., 2020). But most EST-SSR markers are byproducts of stress experiments. However, during the development of microsatellite markers of reef-building corals, coral bleaching is induced by heating, which causes the symbiotic zooxanthellae in the coral to expel from the coral. After coral bleaching, RNA may be partially degraded, which is not conducive to transcriptome sequencing. Therefore, RAD-seq is an advantageous method for coral to develop microsatellite primers.

Conclusion

In this study, the large-scale development of SSR molecular markers of *M. digitata* was carried out through RAD-seq sequencing data, and the sequence characteristics and distribution rules of different motifs of coral SSR loci were analyzed and summarized. Twenty-one pairs of stable polymorphic primers were screened from nine randomly selected coral samples. The acquisition of these microsatellites has laid a foundation for the development of highly polymorphic microsatellite primers to study the genetic diversity, and population genetic structure of populations of *M. digitata* in the future. *M. digitata* is a non-model organism. This study further demonstrates that screening SSRs from high-throughput data is a fast and effective method for discovering SSRs in non-model organisms.

Data availability statement

Author contributions

Investigation, JS, YL, SC, ZC, YW, JS, ZW and DW. Performed the experiments, JS, YL and YW. Writing-original draft preparation, JS and YL. Writing-review and editing, JS, YL, SC, ZC, YW, JS, ZW and DW. All authors have read and agreed to the published version of the manuscript.

Funding

Conflict of interest

The authors declare that the research was conducted in the absence of any commercial or financial relationships that could be construed as a potential conflict of interest.

Publisher's note

All claims expressed in this article are solely those of the authors and do not necessarily represent those of their affiliated organizations, or those of the publisher, the editors and the reviewers. Any product that may be evaluated in this article, or claim that may be made by its manufacturer, is not guaranteed or endorsed by the publisher.

References

Andrews, K. R., Good, J. M., Miller, M. R., Luikart, C., and Hohenlohe, P. A. (2016). Harnessing the power of RADseq for ecological and evolutionary genomics. *Nat. Rev. Genet.* 17 (2), 81. doi: 10.1038/nrg.2015.28

Beedessee, G., Hisata, K., Roy, M. C., Satoh, N., and Shoguchi, E. (2015). Multifunctional polyketide synthase genes identified by genomic survey of the symbiotic dinoflagellate, *Symbiodinium minutum.* . *BMC Genomics* 16 (1), 1–11. doi: 10.1186/s12864-015-2195-8

Cai, L., Yu, L. J., Chen, X. Q., Ye, H. X., Chen, L., and Li, J. J. (2015). A preliminary screening and characteristic analysis of microsatellite markers from transcriptome sequences in mugilogobius chulae. *Biotechnol. Bull.* 31, 146–151. doi: 10.13560/j.cnki.biotech.bull.1985.2015.09.020

Catchen, J. M., Amores, A., Hohenlohe, P., Cresko, W., and Postlethwait, J. H. (2011). Stacks: building and genotyping loci *de novo* from short-read sequences. *G3: Genes| genomes| Genet.* 1 (3), 171–182. doi: 10.1534/g3.111.000240

Chao, K. X., Wu, C. J., Li, J., Wang, W. L., Wang, B. T., and Li, Q. (2022). Genetic analysis of adult plant, quantitative resistance to stripe rust in wheat landrace wudubaijian in multi-environment trials. *J. Integr. Agric.* 21 (8), 2305–2318. doi: 10.1016/S2095-3119(21)63876-5

Chen, J., Li, R., Xia, Y., Bai, G., Guo, P., Wang, Z., et al. (2017). Development of EST-SSR markers in flowering Chinese cabbage (Brassica campestris l. ssp. chinensis var. utilis tsen et Lee) based on *de novo* transcriptomic assemblies. *PloS One* 12, e0184736. doi: 10.0.5.91/journal.pone.0184736

Chen, S., Zhou, Y., Chen, Y., and Gu, J. (2018). Fastp: an ultra-fast all-in-one FASTQ preprocessor. *Bioinformatics* 34 (17), i884–i890. doi: 10.1093/bioinformatics/bty560

Douglas, A. E. (2003). Coral bleaching–how and why? *Mar. pollut. Bull.* 46 (4), 385–392. doi: 10.1016/S0025-326X(03)00037-7

Doyle, J. J., and Doyle, J. L. (1987). A rapid DNA isolation procedure from small quantities of fresh leaf tissues. *Phytochemical Bulletin Botanical Soc. America* 19, 11–15.

Duan, Y. F., Zhang, Z., Li, J. T., Li, J., and Liu, P. (2016). Bioinformatics and microsatellite sequences analysis of EST sequence in ridge tail shrimp exopalaemon carinicauda. *Fisheries Sci.* 35 (5), 562–567.

Excoffier, L., and Lischer, H. E. (2010). Arlequin suitever 3.5: a new series of programs to perform population genetics analyses under Linux and windows. *Mol. Ecol. Resour.* 10, 564–567. doi: 10.1111/j.1755-0998.2010.02847.x

Fan, M., Zhang, X., Nagarajan, R., Zhai, W., Rauf, Y., Jia, H., et al. (2023). Natural variants and editing events provide insights into routes for spike architecture modification in common wheat. *Crop J.* 11 (1), 148–156. doi: 10.1016/j.cj.2022.04.009

Gleason, D. F., and Wellington, G. M. (1993). Ultraviolet and coral bleaching. *Nature* 365 (28), 836–838.

Gonzalez-Ibeas, D., Blanca, J., Roig, C., González-To, M., Picó, B., Truniger, V., et al. (2007). MELOGEN: an EST database for melon functional genomics. *BMC Genomics* 8, 306. doi: 10.1186/1471-2164-8-306

Gu, Q. Y., Li, H. G., Qian, J. G., Liu, J. G., Shi, Y. F., He, K., et al. (2017). Species composition and distribution of scleractinia coral in the port of hainan dazhou island. *Natural Sci. J. Hainan Univ.* 35, 366–371. doi: 10.0.5.91/journal.pone.0184736

Guo, R., Chen, H. Z., Zhuang, T. Y., Xiong, C. L., Zheng, Y. Z., Fu, Z. M., et al. (2018). Exploitation of SSR markers for *Apis mellifera ligustica* based on transcriptome data. *J. Anhui Agric. Univ.* 45, 404–408. doi: 10.13610/j.cnki.1672-352x.20180620.015

He, F. L., Dong, W. Q., Qiu, Z. Y., Jiang, H. P., Liu, L. L., Chen, Q., et al. (2022). Development of polymorphic SSR markers in Chinese water chestnut based on RAD-seq. *Mol. Plant Breed.* 20, 210–217. doi: 10.13271/j.mpb.020.000210

He, D., Zhang, J., Zhang, X., He, S., Xie, D., Liu, Y., et al. (2020). Development of SSR markers in paeonia based on *De novo* transcriptomic assemblies. *PloS One* 15 (1), e0227794. doi: 10.1371/journal.pone.0227794

Hou, J. (2018). *Genetic structure and connectivity of scleractinian coral porites lutea around hainan island.* Master thesis. (Haikou: Hainan University).

Huang, W. J., Guo, X. Z., Zhang, Z. H., Dong, Q., Xiong, X. M., and Gao, Z. X. (2022). Analysis of microsatellite in the entire grass carp (*Ctenopharyngodon idella*) genome and the application in parentage identification. *J. Fisheries China* 46, 161–172.

Huang, J., Zhou, Y., Liu, Y. Z., Zhu, D., Song, X. H., Chen, B. Q., et al. (2015). Characteristics of microsatellites in *Arborophila rufipectus* genome sequences using 454 GS FLX. *Sichuan J. Zoology* 34, 8–14.

Hughes, T. P., Barnes, M. L., Bellwood, D. R., Cinner, J. E., Cumming, G. S., Jackson, J. B. C., et al. (2017). Coral reefs in the anthropocene. *Nature* 546 (7656), 82–90. doi: 10.1038/nature22901

Hughes, T. P., Huang, H., and Young, M. A. (2012). The wicked problem of china's disappearing coral reefs. *Conserv. Biol.* 27 (2), 261–269. doi: 10.1111/j.1523-1739.2012.01957.x

Jia, S. W., Liu, P., Li, J., Li, J. T., and Pan, L. Q. (2013). Isolation and characterization of polymorphic microsatellite loci in the ridgetail white prawn exopalaemon carinicauda. *Genet. Mol. Res.* 12 (3), 2816–2820. doi: 10.4238/2013.August.8.1

Jia, S. W., and Zhang, M. L. (2019). Pleistocene climate change and phylogeographic structure of the gymnocarpos przewalskii (Caryophyllaceae) in the northwest China: evidence from plastid DNA, ITS sequences, and microsatellite. *Ecol. Evol.* 9, 5219–5235. doi: 10.1002/ece3.5113

Jo, E., Lee, S. J., Choi, E., Kim, J., Lee, S. G., Lee, J. H., et al. (2021). Whole genome survey and microsatellite motif identification of artemia franciscana. *Bioscience Rep.* 41 (3), 1–6. doi: 10.1042/BSR20203868

Karcı, H., Paizila, A., Topçu, H., Ilikçioğlu, E., and Kafkas, S. (2020). Transcriptome sequencing and development of novel genic SSR markers from pistacia vera l. *Front. Genet.* 11, 1021. doi: 10.3389/fgene.2020.01021

Li, F., Chen, D., Li, Y., Li, S., Hou, J., Wang, D., et al. (2020). Development of microsatellite markers for the hermatypic coral *Porites lutea*. *Genomics Appl. Biol.* 40, 2513–2521. doi: 10.5376/ijms.2020.10.0003

Li, W. J., Li, Y. Z., Du, L. M., Huang, J., Shen, Y. M., Zhang, X. Y., et al. (2014). Comparative analysis of microsatellite sequences distribution in the genome of giant panda and polar bear. *Sichuan J. Zoology* 33, 874–878.

Li, H., Liu, D. C., Xu, R. R., Hou, L., Wang, T. Q., Liu, Z. H., et al. (2021). Development and identification of SSR markers based on RAD-seq of lonicera japonica. *J. Beijing Forestry Univ.* 43 (6), 108–117.

Lin, S., Cheng, S., Song, B., Zhong, X., Lin, X., Li, W., et al. (2015). The *Symbiodinium kawagutii* genome illuminates dinoflagellate gene expression and coral symbiosis. *Science* 350 (6261), 691–694.

Liu, H. J., Zhang, Y. L., Wang, Z., Su, Y. J., and Wang, T. (2021). Development and application of EST-SSR markers in *Cephalotaxus oliveri* from transcriptome sequences. *Front. Genet.* 12, 759557. doi: 10.3389/fgene.2021.759557

Luo, Y., Huang, W., Yu, K., Li, M., Chen, B., Huang, X. Y., et al. (2022). Genetic diversity and structure of tropical *Porites lutea* populations highlight their high adaptive potential to environmental changes in the south china sea. *Front. Mar. Sci.* 9, 791149. doi: 10.3389/fmars.2022.791149

Luo, Y. Q., Huang, W., Yu, K. F., Li, M., Wu, Q., Wang, Y. H., et al. (2020). Development of microsatellite in *Pocillopora damicornis* using high-throughput sequencing. *J. Guangxi Univ.* 45, 958–965. doi: 10.13624/j.cnki.issn.1001-7445.2020.0958

Luo, M., Zhang, H., Bin, S., and Lin, J. (2014). High-throughput discovery of SSR genetic markers in the mealybug, phenacoccus solenopsis (Hemiptera: pseudococcidae), from its transcriptome database. *Acta Entomologica Sin.* 57 (4), 395–400. doi: 10.16380/j.kcxb.2014.04.005

Ni, S. S., Yang, Y., Liu, S. F., and Zhuang, Z. M. (2018). Microsatellite analysis of patinopecten yessoensis using next-generation sequencing method. *Prog. Fishery Sci.* 39 (1), 107–113.

Nie, H., Cao, S. S., Zhao, M. L., and Du, L. F. (2017). Comparative analysis of microsatellite distributions in genomes of boa constrictor and protobothrops mucrosquamatus. *Sichuan J. Zoology* 36 (6), 639–648.

Peakall, R., and Smouse, P. E. (2006). GENALEX 6: genetic analysis in excel. population genetic software for teaching and research. *Mol. Ecol. Resour.* 6, 288–295. doi: 10.1111/j.1471-8286.2005.01155.x

Peng, Y., Li, J., Wang, T., Zhang, K., Ning, X. H., Ji, J., et al. (2022). Preliminary study on distribution characteristics and positioning of microsatellites in whole genome of *Pelteobagrus vachelli*. *South China Fisheries Sci.* 18, 91–98.

Qi, W. H., Jiang, X. M., Du, L. M., Xiao, G. S., Hu, T. Z., Yue, B. S., et al. (2015). Genome-wide survey and analysis of microsatellite sequences in bovid species. *PloS One* 10 (7), e0133667. doi: 10.1371/journal.pone.0133667

Qi, W. H., Yan, C. C., Xiao, G. S., Zhang, W. Q., and Yue, B. S. (2016). Distribution regularities and bioinformatics analysis of microsatellite in the whole genomes of goat and tibetan antelope. *J. Sichuan Univ. (Natural Sci. Edition)* 53, 937–944.

Qu, Z. W., Song, H. M., Wang, X. J., Liu, Y., Mu, X. D., Liu, C., et al. (2019). Preliminary screening and characterization of microsatellite markers in RAD-seq data of datnioides pulcher. *Freshw. Fisheries* 49 (4), 9–15. doi: 10.13721/j.cnki.dsyy.2019.04.002

Ren, F., and Ma, X. H. (2021). Characteristics analysis of SSR markers based on transcriptomic sequenceing of *Placocheilus cryptonemus*. *Jiyinzuxue yu Yingyong Shengwuxue (Genomics Appl. Biology)* 40, 1055–1060. doi: 10.13417/j.gab.040.001055

Ruiz-Ramos, D. V., and Baums, I. B. (2014). Microsatellite abundance across the anthozoa and hydrozoa in the phylum cnidaria. *BMC Genomics* 15 (1), 1–17. doi: 10.1186/1471-2164-15-939

Shoguchi, E., Shinzato, C., Hisata, K., Satoh, N., and Mungpakdee, S. (2015). The large mitochondrial genome of symbiodinium minutum reveals conserved noncoding sequences between dinoflagellates and apicomplexans. *Genome Biol. Evol.* 7 (8), 2237–2244. doi: 10.1093/gbe/evv137

Shoguchi, E., Shinzato, C., Kawashima, T., Gyoja, F., Mungpakdee, S., Koyanagi, R., et al. (2013). Draft assembly of the *Symbiodinium minutum* nuclear genome reveals dinoflagellate gene structure. *Curr. Biol.* 23 (15), 1399–1408. doi: 10.1016/j.cub.2013.05.062

Song, C. Y., Feng, Z. Y., Li, C. H., Sun, Z. C., Gao, T. X., Song, N., et al. (2020). Profile and development of microsatellite primers for acanthogobius ommaturus based on high-throughput sequencing technology. *J. Oceanol. Limnol.* 1–11. doi: 10.1007/s00343-019-9154-1

Song, L. L., Wang, D. D., and Zhou, X. J. (2022). Microsatellites characterization analysis of clematis heracleifolia using high throughput sequencing method. *Mol. Plant Breed.* 20, 1087–1094. doi: 10.13271/j.mpb.020.001087

Su, D. J. (2017). *Genetic structure and connectivity of scleractinian coral galaxea fascicularis around hainan island* (Hainan University).

Su, M. Y., Yang, W. S., Tang, R. Y., Xu, J. J., Wang, T., and Yin, S. W. (2021). Microsatellite distribution in the whole genome of ageneiosus marmoratus. *J. Nanjing Normal Univ. (Engineering Technol. Edition)* 21, 65–71.

Sun, Y., Guo, B. Y., QI, Z. P., Chen, Y., Tang, Z. R., and Liu, S. B. (2019). Analysis on ssr and snp information in transcriptome sequences of *Sepiella japonica*. *J. Zhejiang Ocean Univ. (Natural Science)* 38, 100–106.

Sun, X., Liu, D., Zhang, X., Li, W., Liu, H., Hong, W., et al. (2013). SLAF-seq: an efficient method of large-scale *de novo* SNP discovery and genotyping using high-throughput sequencing. *PloS One* 8 (3), e58700. doi: 10.1371/journal.pone.0058700

Tang, R. Y., Su, M. Y., Yang, W. S., Xu, J. J., Wang, T., and Yin, S. W. (2022). Analysis of microsatellite distribution characteristics in the channel catfish (*Ictalurus punctatus*) genome. *Prog. Fishery Sci.* 43 (2), 89–97. doi: 10.19663/j.issn2095-9869.20210126002

Tu, F. Y., Liu, J., Han, W. J., Huang, T., and Huang, X. F. (2018). Analysis of microsatellite distribution characteristics in the entire genome of *Macaca fascicularis*. *Chin. J. Wildlife* 39, 400–4404. doi: 10.19711/j.cnki.issn2310-1490.2018.02.032

Van Oosterhout, C., Hutchinson, W. F., Wills, D. P. M., and Shipley, P. (2004). MICROCHECKER: software for identifying and correcting genotyping error in microsatellite data. *Mol. Ecol. Notes* 4, 535–538. doi: 10.1111/j.1471-8286.2004.00684.x

Wan, D. M., Han, M., Li, C. A., and He, Y. X. (2016). Development of microsatellite in marsh tit *Parus palustris* using illumina MiSeq. *J. Liaoning Univ.* 43, 252–257. doi: 10.16197/j.cnki.lnunse.2016.03.012

Wang, Q. Y., Guo, W. J., Cheng, W. W., Deng, G. Q., Xu, H. L., and Xia, R. L. (2021). Isolation of microsatellite markers for pelteobagrus vachellii based on RAD sequencing. *Fisheries Sci. & Technol. Inf.* 48, 250–254. doi: 10.16446/j.fsti.20200700123

Wang, Y. K., Hu, Y., and Zhang, T. Z. (2014). Current status and perspective of RAD-seq in genomic research. *Hereditas (Beijing)* 36 (1), 41–49.

Wang, Z. L., Huang, J., Du, L. M., Li, W. J., Yue, B. S., and Zhang, X. Y. (2013). Comparison of microsatellites between the genomes of tetranychus urticae and ixodes scapularis. *Sichuan J. Zoology* 32, 481–486.

Wang, S., Meyer, E., McKay, J. K., and Matz, M. V. (2012). 2b-RAD: a simple and flexible method for genome-wide genotyping. *Nat. Methods* 9 (8), 808. doi: 10.1038/nmeth.2023

Wang, Y. R., Yang, W., Ren, X. L., Jiang, D. N., Deng, S. P., Chen, H. P., et al. (2020). Distribution patterns of microsatellites and development of polymorphic markers from *Scatophagus argus* genome. *J. Guangdong Ocean Univ.* 40, 7–14.

Wang, X. T., Zhang, Y. J., Xiu, H. E., Mei, T., and Chen, B. (2016). Identification, characteristics and distribution of microsatellites in the whole genome of anopheles sinensis (diptera: culicidae). *Acta Entomologica Sin.* 59, 1058–1068. doi: 10.16380/j.kcxb.2016.10.004

Wu, Z. M., Gao, P., and Wen, J. B. (2016). Characteristic analysis of microsatellite in eucryptorrhynchus chinensis transcriptome. *J. Environ. Entomology* 38 (5), 979–983.

Wu, Q., Huang, W., Chen, B., Yang, E., Meng, L., Chen, Y., et al. (2021). Genetic structure of *Turbinaria peltata* in the northern south China Sea suggest insufficient genetic adaptability of relatively high-latitude scleractinian corals to environment stress. *Sci. total Environ.* 775, 145775. doi: 10.1016/j.scitotenv.2021.145775

Xing, W., Liao, J., Cai, M., Xia, Q., Liu, Y., Zeng, W., et al. (2017). *De novo* assembly of transcriptome from rhododendron latoucheae franch. using illumina sequencing and development of new EST-SSR markers for genetic diversity analysis in rhododendron. *Tree Genet. Genomes* 13 (53), 1–15. doi: 10.1007/s11295-017-1135-y

Xu, J. J., Bi, Y. H., Cheng, J. H., Xing, X. M., Ji, J., Wang, T., et al. (2021b). Study on distribution characteristics of whole genome microsatellite of *Eriocheir sinensis*. *Jiyinzuxue yu Yingyong Shengwuxue (Genomics Appl. Biology)* 40, 2422–2429. doi: 10.13417/j.gab.040.002422

Xu, J. J., Zheng, X., Li, J., Yin, S. W., and Wang, T. (2020). Distribution characteristics of whole genome microsatellite of *Pelteobagrus fulvidraco*. jiyinzuxue yu yingyong shengwuxue. *(Genomics Appl. Biology)* 39, 5488–5498. doi: 10.13417/j.gab.039.005488

Xu, J. J., Zheng, X., Zhang, X. Y., Wang, T., and Yin, S. W. (2021a). Analysis of distribution characteristics of microsatellites in four genomes of puffer fish. *Jiyinzuxue yu Yingyong Shengwuxue (Genomics Appl. Biology)* 40, 1441–1451. doi: 10.13417/j.gab.040.001441

Yang, X. L. (2013). *Development of microsatellite markers in platygyra acuta and analysis of genetic diversity of populations from some scleractinian*. Master Thesis. (Zhanjiang: Guangdong Ocean University).

Yang, W. S., Tang, R. Y., Su, M. Y., Xu, J. J., Wang, T., and Yin, S. W. (2021). Analysis of microsatellite distribution characteristics in the whole genome of *Bagarius yarrelli*. *J. Nanjing Normal Univ. (engineering Technol. edition)* 21, 62–68.

Yuan, Y., Zhang, L. F., Wu, G. X., and Zhu, J. Y. (2014). High-throughput discovery microsatellites in *Tomicus yunnanensis* (Coleoptera: scolytinae). *J. Environ. Entomology* 36, 166–170.

Zhang, P., Zhou, X., Pang, B., Tan, Y., Chang, J., and Gao, L. (2016). High-throughput discovery of microsatellite markers in galeruca daurica (Coleoptera: chrysomelidae) from a transcriptome database. *Chin. J. Appl. Entomology* 53 (5), 1058–1064.

Zhou, H. Y., Yao, X. M., Li, L., Geng, T. N., and Zhang, Y. (2017). Scleractinian coral community structure and distribution in the coastal waters surrounding hainan island. *Biodiversity Sci.* 25 (10), 1123–1130. doi: 10.17520/biods.2017079

Zhu, J., Wu, G., and Yang, B. (2013). High-throughput discovery of SSR genetic markers in the yellow mealworm beetle, tenebrio molitor (Coleoptera: tenebrionidae), from its transcriptome database. *Acta Entomologica Sin.* 56 (7), 724–728. doi: 10.16380/j.kcxb.2013.07.012